



Synthesis, Characterization, and Catalytic Properties of Magnetic Fe₃O₄@FU: A Heterogeneous Nanostructured Mesoporous Bio-Based Catalyst for the Synthesis of Imidazole Derivatives

Maryam Banazadeh, Sara Amirnejat and Shahrzad Javanshir*

Heterocyclic Chemistry Research Laboratory, Chemistry Department, Iran University of Science and Technology, Tehran, Iran

OPEN ACCESS

Edited by:

Ruquan Ye,
City University of Hong Kong,
Hong Kong

Reviewed by:

Viorica Parvulescu,
Romanian Academy, Romania
Shilpi Ghosh,
University of Marburg, Germany

*Correspondence:

Shahrzad Javanshir
shjavan@iust.ac.ir

Specialty section:

This article was submitted to
Catalysis and Photocatalysis,
a section of the journal
Frontiers in Chemistry

Received: 18 August 2020

Accepted: 07 October 2020

Published: 01 December 2020

Citation:

Banazadeh M, Amirnejat S and
Javanshir S (2020) Synthesis,
Characterization, and Catalytic
Properties of Magnetic Fe₃O₄@FU: A
Heterogeneous Nanostructured
Mesoporous Bio-Based Catalyst for
the Synthesis of Imidazole Derivatives.
Front. Chem. 8:596029.
doi: 10.3389/fchem.2020.596029

In this protocol, Fucoidan (FU), a fucose-rich sulfated polysaccharide extracted from brown algae *Fucus vesiculosus* was used for *in situ* preparation of magnetic Fe₃O₄@FU. Nanoco magnetic properties of Fe₃O₄@FU were investigated by energy dispersive X-ray (EDX) spectroscopy, X-ray diffraction (XRD), Fourier transform infrared spectroscopy (FT-IR), field emission scanning electron microscopy (FESEM), transmission electron microscopy (TEM), Brunauer–Emmett–Teller (BET) adsorption method, and vibrating sample magnetometer (VSM). The catalytic activity of Fe₃O₄@FU was employed for the synthesis of tri- and tetra-substituted imidazoles through three- and four-component reactions respectively, between benzyl, aldehydes, NH₄OAc and benzyl, aldehydes, NH₄OAc, and amine under reflux in ethanol. It is worth nothing that excellent yields, short reaction times, chromatography-free purification, and environmental friendliness are highlighted features of this protocol.

Keywords: fucoidan, heterogeneous catalyst, imidazoles, superparamagnetic iron oxide nanoparticles, sulfated polysaccharides

INTRODUCTION

Through extensive applications and potential in the chemical industry and preservation of the environment, the recently supported solid nanocatalysis has been faced with various attentions in catalysis science and technology (Amirnejat et al., 2013; Fereshteh and Shahrzad, 2020). To overcome the difficulty of catalyst separation, some magnetic heterogeneous catalysts with unique features and advanced functionalities suitable for a range of applications, including biological and environmental applications have been made (Pourian et al., 2018; Zaheri et al., 2018). The magnetic materials have gained more attention due to their combined physicochemical characteristics such as high surface area, high thermal and chemical stability, excellent biocompatibility and biodegradability, and efficient super magnetic behavior (Dolatkhah et al., 2018; Piri et al., 2019).

Natural biopolymers as an effective tool have given rise to a new method of producing degradable materials. Meanwhile, marine polysaccharides exhibit a vast variety of structures and could be considered as a novel natural source (Dekamin et al., 2016; Alipour et al., 2018; Dolatkhah et al., 2019). Nanomaterials based on marine polysaccharides have been considered as one of

the most important topics of research in recent years, especially in chemical and bio-based research, due to biocompatibility and biodegradability, cheapness, non-toxicity, and abundance (Hemmati et al., 2016; Amirnejat et al., 2020a,b,c). Fucoidan refers to a type of polysaccharide which contains substantial percentages of L-fucose and sulfated ester groups, mainly derived from brown seaweed which has been extensively studied due to its numerous interesting biological activities (Gomez-Zavaglia et al., 2019; Zayed and Ulber, 2019, 2020).

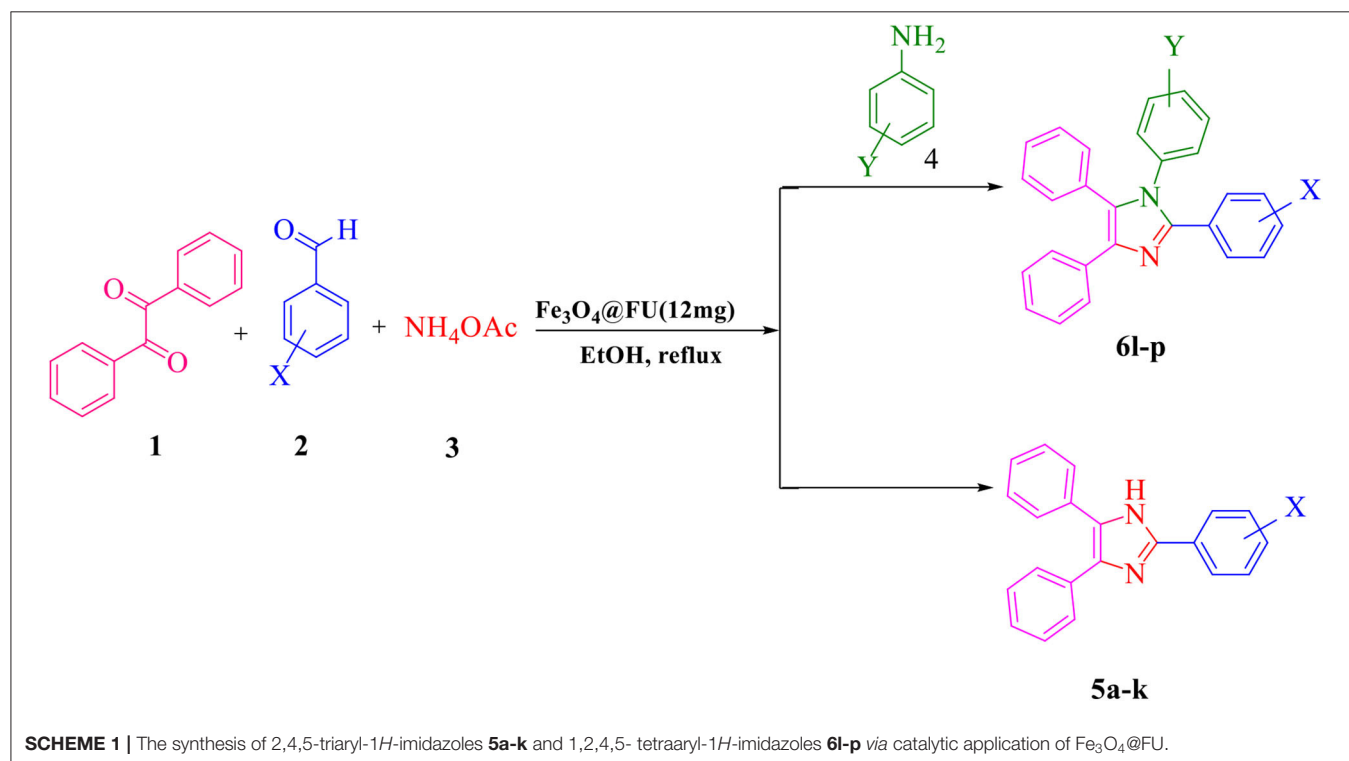
In recent decades, it has been extensively represented that multi-component reaction (MCR) is an ideal tool for creating molecular diversity and complexity (Graebin et al., 2019). Meanwhile imidazoles, polar in nature and with a five-member ring structure, are one of the most important compounds showing a wealthy source of biologically important features such as inhibitors, fungicides, herbicides plant, anti-inflammatory, anticancer, antimicrobial, analgesic, and anti-tubercular activity (Shalini et al., 2010; Varzi and Maleki, 2019). Numerous approaches have been developed for the synthesis of 1,2,4,5-tetra-substituted imidazoles, which can be prepared by a four-component cyclo condensation consisting of aldehyde, benzil, a primary amine and ammonium acetate in the presence of different catalysts such as $\text{BF}_3 \cdot \text{SiO}_2$ (Sadeghi et al., 2008), and silica gel/ NaHSO_4 (Karimi et al., 2006), while other main components are achieved by synthesis of tri-substituted imidazoles by the condensation of benzil derivatives, aryl aldehydes, and ammonium acetate catalyzed by different catalysts such as ZrCl_4 (Shitole et al., 2015), sulfanilic acid (Gadekar et al., 2009), and chitosan (Zheng et al., 2019). However, some of these methodologies have

some drawbacks, such as low yields, long reaction times, severe reaction conditions, and work up procedure. Herein, we report the *in situ* synthesis of a novel eco-friendly magnetic heterogeneous catalyst $\text{Fe}_3\text{O}_4@FU$ for the synthesis of tri- and tetra-substituted imidazoles under reflux condition in ethanol (**Scheme 1**). Easy work up and separation, high product yields and short reaction times made this method effective and advantageous.

EXPERIMENTAL

Materials and Methods

All solvents and chemicals were purchased from Merck and Aldrich. All reactions and the purity of the products were monitored by thin-layer chromatography (TLC) using aluminum plates coated with silica gel F254 plates (Merck) using ethyl acetate and n-hexane as eluents. UV light with a wavelength of 254 nm was used for the detection of products. By using an Electro thermal 9100, melting points were determined in open capillaries. IR spectra were run on a 400s Shimadzu FTIR Spectrophotometer (as KBr pellets). ^1H and ^{13}C NMR spectra were recorded on a 500 MHz Bruker Avance DRX Spectrometer instrument using TMS as an internal standard and CDCl_3 , $\text{DMSO}-d_6$ as a solvent. The XRD patterns were obtained on an X-ray diffractometer (Holland, Philips Xpert, Co K, radiation, $\lambda = 0.178897$ nm). A Field Emission Scanning Electron Microscope (FE-SEM) with 15 KV, Mira3, Tescan), Thermal Gravimetric Analysis (TGA D-32609 from Hullhorst), and Transmission electron microscope (TEM, Philips -CM120, 100 KV) were used. An ultrasonic probe watt ultrasonic homogenizer 400 from



Topsonics Co was used in room temperature for optimization of the reaction.

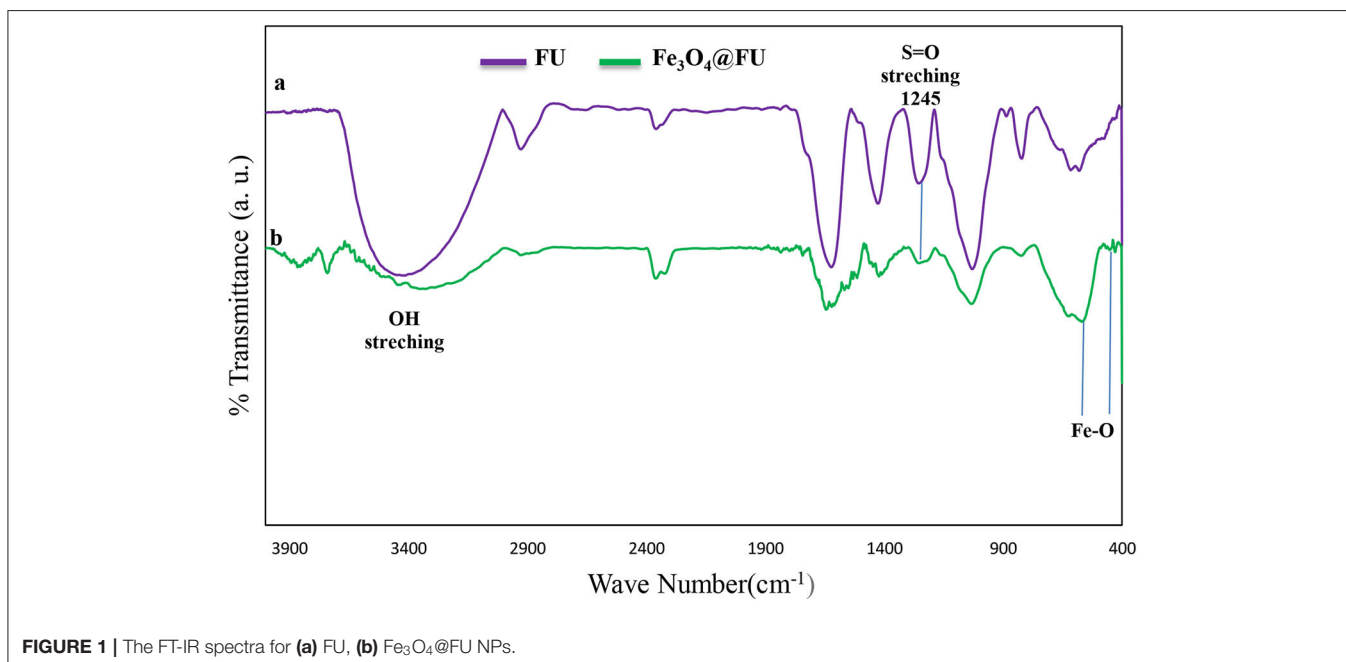
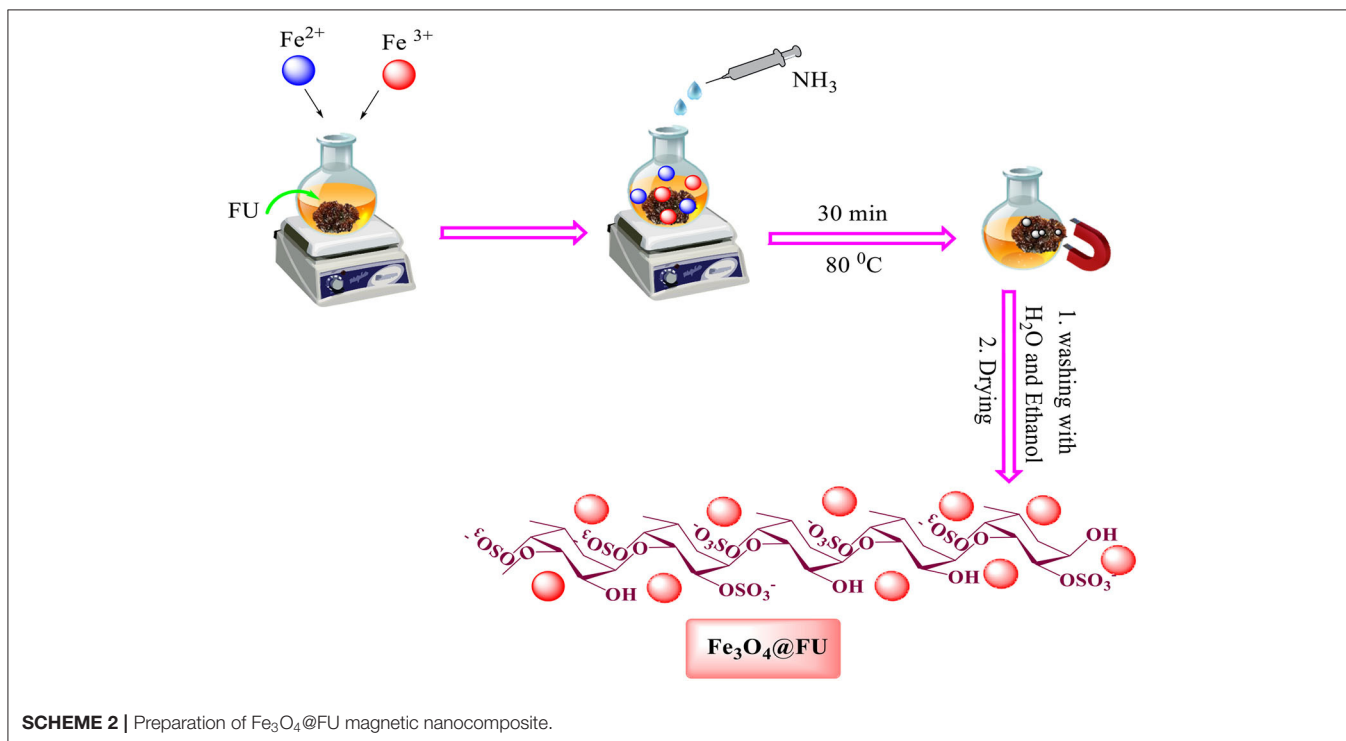
the suspension was centrifuged at 4,000 rpm for 15 min and the resulting powder was dried at 50°C for 1 h.

Preparations of Fucoidan Powder

2.5 gr of algae *Fucus vesiculosus* was finely ground by a ball mill for 5 min and was placed in a round bottom 200 ml flask containing 100 ml of 96% ethanol, and was stirred for 12 h. Then,

Synthesis of Magnetic Fe₃O₄@FU Nanocomposite

For the preparation of the Fe₃O₄@FU, 0.2 g of fucoidan powder, FeCl₂·4H₂O (2 g, 0.01 mol) and (5.5 g, 0.02 mol) of FeCl₃ were



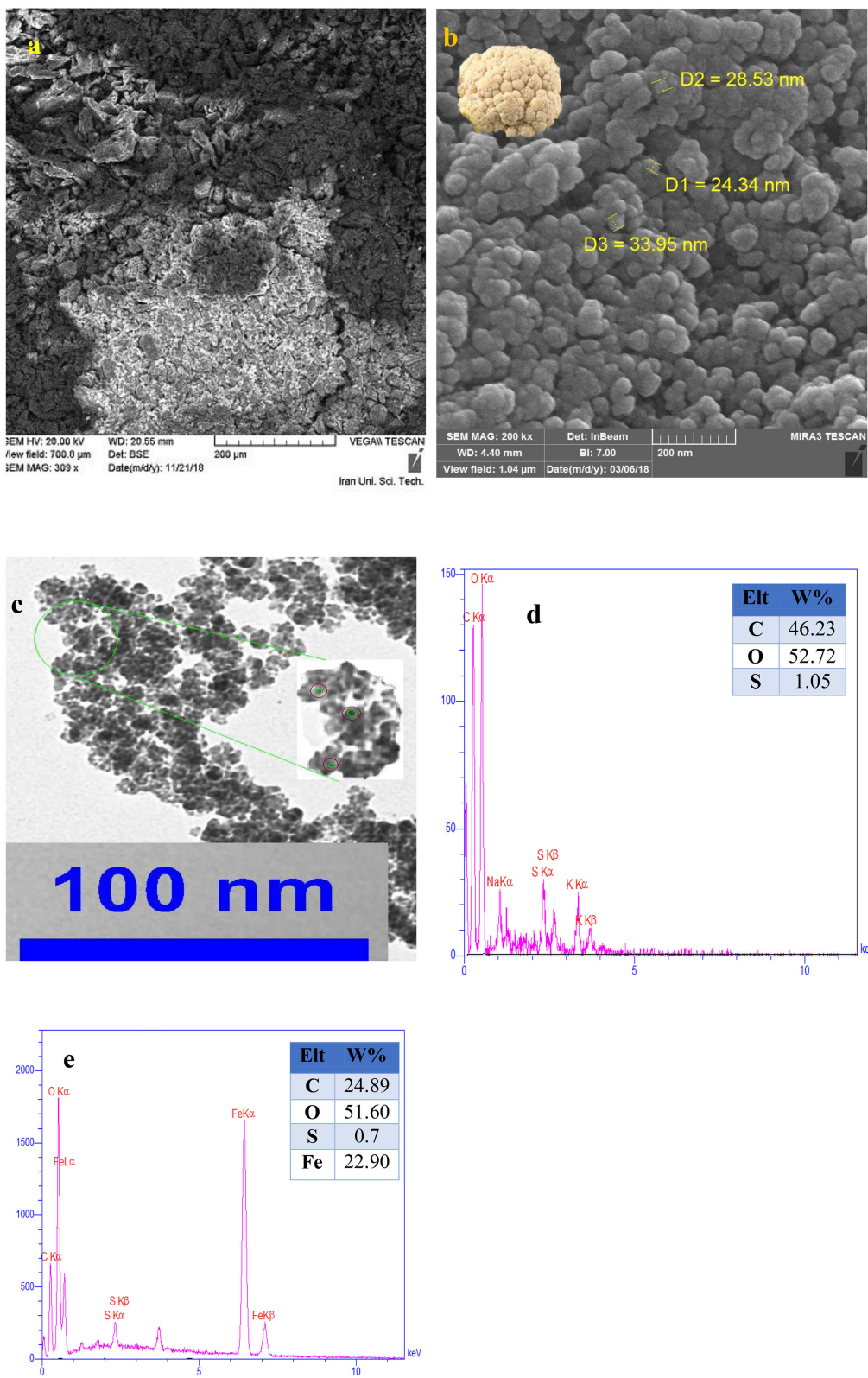


FIGURE 2 | SEM images of **(a)** FU, **(b)** $Fe_3O_4@FU$, and **(c)** TEM images of $Fe_3O_4@FU$ NPs. EDX analysis of **(d)** FU, and **(e)** $Fe_3O_4@FU$ NPs.

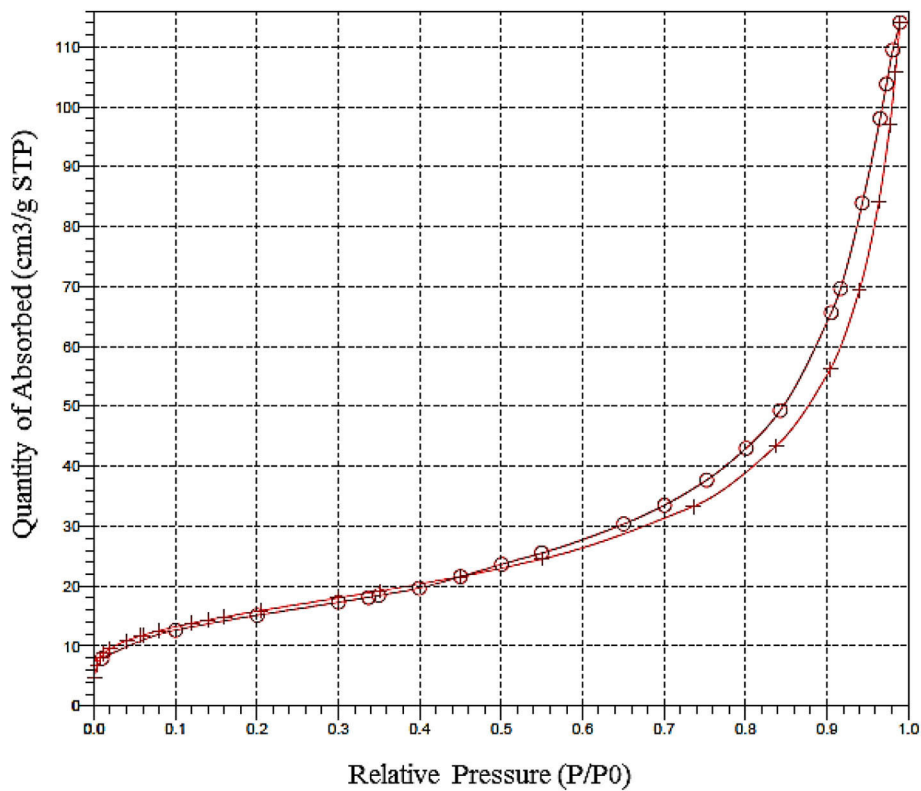


FIGURE 3 | BET curve of Fe₃O₄@FU NPs.

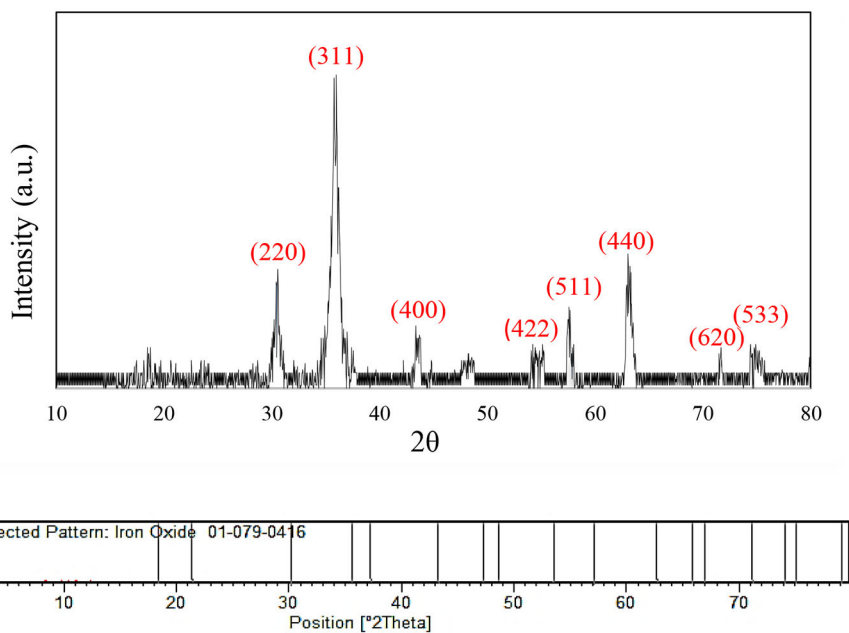


FIGURE 4 | XRD patterns of Fe₃O₄@FU NPs.

used. $6\text{H}_2\text{O}$ was dissolved in 100 ml of distilled water. Then the mixture was vigorously stirred under a nitrogen atmosphere at 80°C for 15 min to reach a uniform solution. The pH of the solution was then adjusted to 12 by the dropwise addition of an aqueous ammonia solution (25%). The mixture was stirred at 80°C for 45 min. The prepared magnetic nanoparticles were separated by an external magnet, finally washed with ethanol and DI, and dried for 6 h at 60°C (Scheme 2).

General Procedure for the Preparation of 2, 4, 5-Trisubstituted Imidazoles Derivatives

A mixture of benzil (210 mg, 1 mmol), aldehydes (1 mmol), NH_4OAc (154 mg, 2 mmol), and $\text{Fe}_3\text{O}_4@FU$ NPs (12 mg) in 3 ml EtOH was stirred under reflux conditions for the appropriate

times. The progress of the reactions was monitored by TLC (eluent: EtOAc / n-hexane, 1: 3). After completion of the reaction, the catalyst was easily separated by an external magnet and then reused as such for the following experiment after being washed with EtOH and dried. The pure products were obtained by recrystallization from hot EtOH and then dried at 60°C for 1 h.

General Procedure for the Preparation of 1, 2, 4, 5-Tetrasubstituted Imidazoles Derivatives

Benzil (210 mg, 1 mmol), aldehydes (1 mmol), NH_4OAc (77 mg, 1 mmol), amine (1 mmol), and $\text{Fe}_3\text{O}_4@FU$ NPs (12 mg) in ethanol (3 mL) was stirred under reflux conditions until completion of the reaction which was monitored by TLC (eluent: EtOAc/n-hexane, 1:3). The catalyst was separated from the mixture by an external magnet, washed and dried for use in the next run. The crude products were filtered and recrystallized from ethanol.

RESULTS AND DISCUSSION

$\text{Fe}_3\text{O}_4@FU$ magnetic nanoparticles as a heterogeneous catalyst were characterized by Fourier transform infrared (FT-IR) spectral analysis. One strong broad band at $3,500\text{ cm}^{-1}$ was attributed to the stretching vibration due to the O-H of fucoidan and water. The appearance of the peak at $1,624\text{ cm}^{-1}$, attributed to significant polysaccharide chains (Figure 1a), is stronger than magnetic fucoidan (Figure 1b). The absorption band at $1,029\text{ cm}^{-1}$ indicated hemiacetal vibration at alcohol and ether functional groups in fucoidan structure. Furthermore, the peak at $1,240\text{--}1,255\text{ cm}^{-1}$ was related to the stretching vibration of S=O from the SO_3H group. The presence of the metal oxide peaks of 570 and 455 cm^{-1} also exhibited in FT-IR of $\text{Fe}_3\text{O}_4@FU$

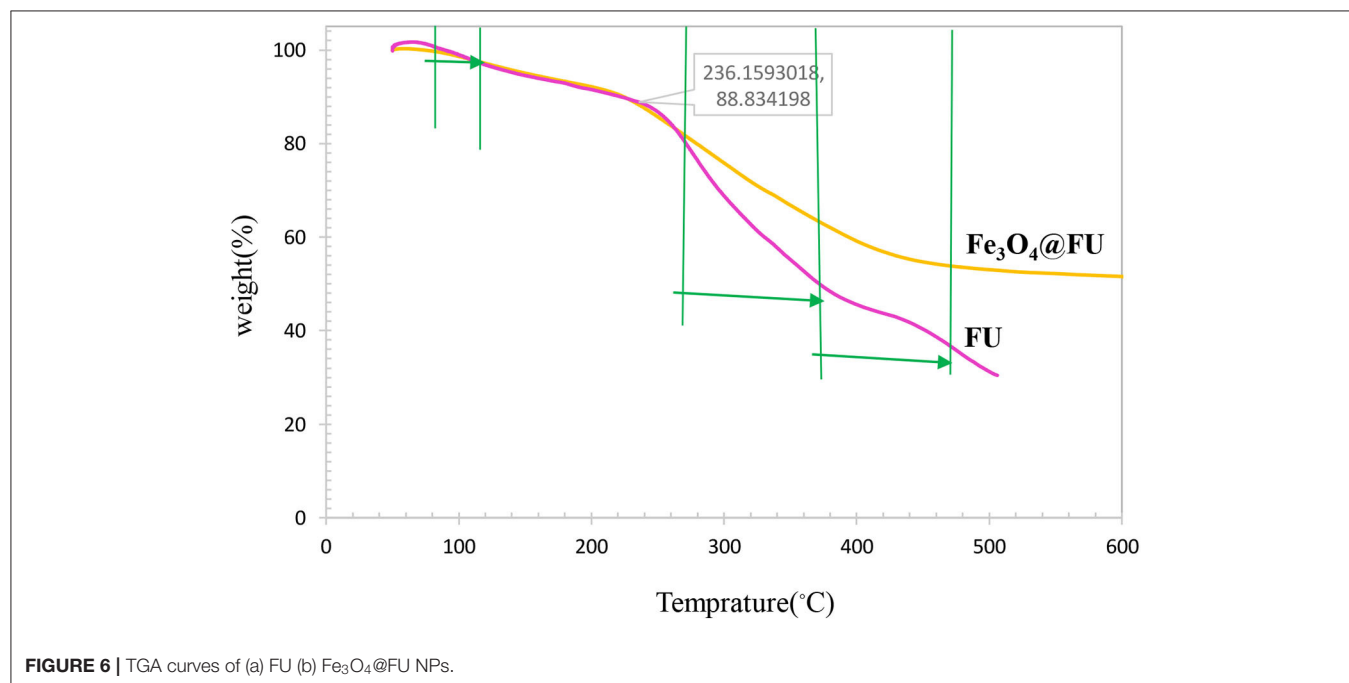
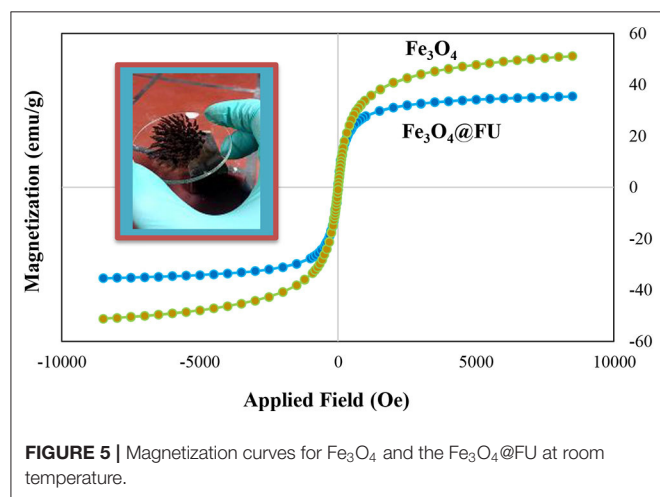
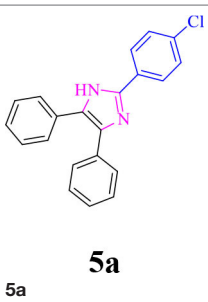
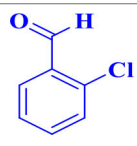
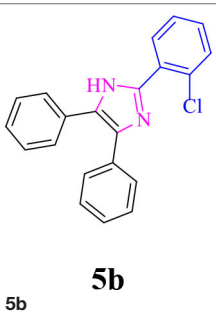


TABLE 1 | Condition optimization for the synthesis of 2,4,5-trisubstituted imidazole (5k)^a.

Entry	Catalyst	Temp. (°C)	Solvent	Catalyst (mg)	Time (min)	Yield (%)
1	-	r.t.	Solvent free	-	24 h	-
2	-	Reflux	Ethanol	-	250	Trace
3	FU	Reflux	Ethanol	12	40	70
4	Fe ₃ O ₄	Reflux	Ethanol	12	40	55
5	Fe ₃ O ₄ @FU	Reflux	Ethanol	12	20	96
6	Fe ₃ O ₄ @FU	Reflux	Ethanol/ Water	12	30	80
7	Fe ₃ O ₄ @FU	r.t.	Ethanol	12	35	75
8	Fe ₃ O ₄ @FU	Reflux	Water	12	40	60
9	Fe ₃ O ₄ @FU	Reflux	CH ₃ CN	12	70	48
10	Fe ₃ O ₄ @FU	Reflux	THF	12	90	40
11	Fe ₃ O ₄ @FU	Reflux	Toluene	12	60	45
12	Fe ₃ O ₄ @FU	Reflux	Ethanol	15	20	96
13	Fe ₃ O ₄ @FU	Reflux	Ethanol	10	30	90
14	Fe ₃ O ₄ @FU	Reflux	Ethanol	5	50	60

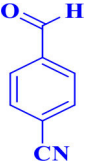
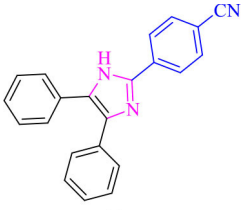
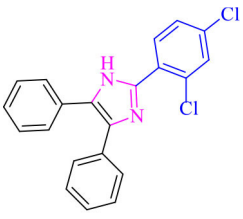
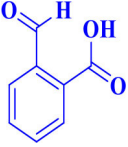
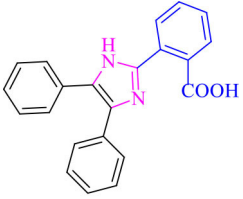
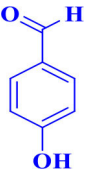
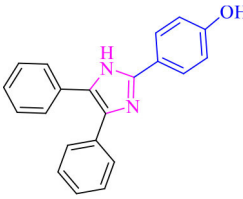
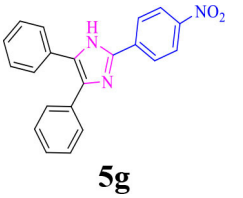
^aReaction conditions: benzaldehyde (1 mmol), benzil (1 mmol), ammonium acetate (2 mmol), solvent (3 ml).

TABLE 2 | Synthesis of 2,4,5-triaryl (5a-k)^a and 1,2,4,5-tetraaryl-1H-imidazoles (6l-p)^b catalyzed by Fe₃O₄@FU nanocomposite.

Entry	R ¹ -ArCHO	R ² -ArNH ₂	Product ^d	Time (min)	Yield ^c (%)	M.p (°C) found/reported
1		-	 5a	12	96	261–262/260–261 (Salimi et al., 2015)
2		-	 5b	20	90	192–194/191–192 (Shaabani et al., 2017)

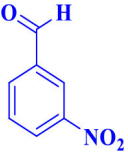
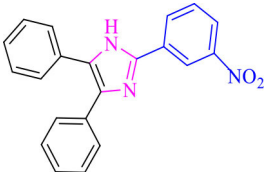
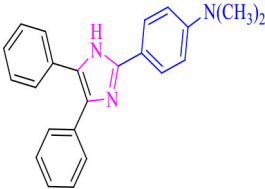
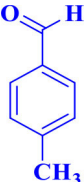
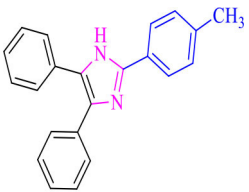
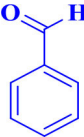
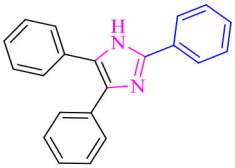
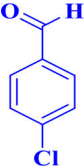
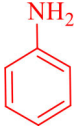
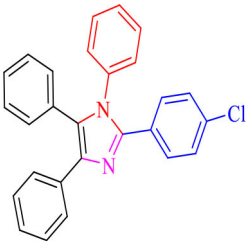
(Continued)

TABLE 2 | Continued

Entry	R ¹ -ArCHO	R ² -ArNH ₂	Product ^d	Time (min)	Yield ^e (%)	M.p (°C) found/reported
3		-	 5c	12	96	248–250/248–250 (Marques et al., 2012)
4		-	 5d	15	91	170–173/171–174 (Amirnejat et al., 2020a)
5		-	 5e	22	90	301–303/300–303 (Amirnejat et al., 2020a)
6		-	 5f	25	88	229–231/230–233 (Momahed Heravi et al., 2019)
7		-	 5g	15	95	195–197/196–198 (Shaabani et al., 2016)

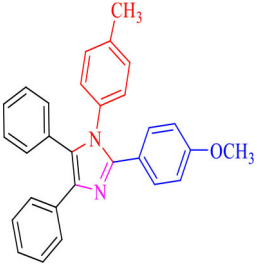
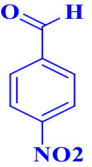
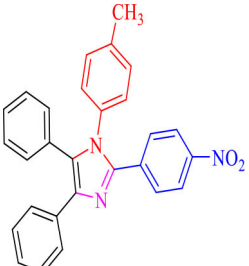
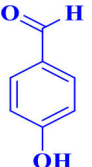
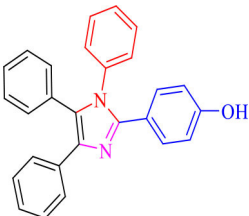
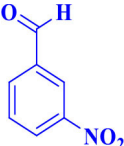
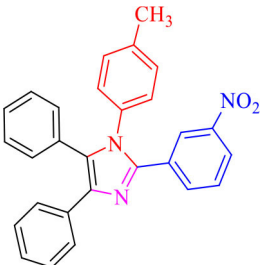
(Continued)

TABLE 2 | Continued

Entry	R ¹ -ArCHO	R ² -ArNH ₂	Product ^d	Time (min)	Yield ^e (%)	M.p (°C) found/reported
8		-	 5h	20	86	314–316/313–315 (Movahed Heravi et al., 2019)
9		-	 5i	25	80	257–259/256–259 (Salimi et al., 2015)
10		-	 5j	30	80	230–232/230–232 (Mirsafaei et al., 2016)
11		-	 5k	20	90	268–270/270 (Shaterian and Ranjbar, 2011)
12			 6l	20	94	157–159/156–158 (Salimi et al., 2015)

(Continued)

TABLE 2 | Continued

Entry	R ¹ -ArCHO	R ² -ArNH ₂	Product ^d	Time (min)	Yield ^c (%)	M.p (°C) found/reported
13			 6m	30	85	175–177/176–178 (Ray et al., 2013)
14			 6n	30	90	230–234/232–236 (Salimi et al., 2015)
15			 6o	35	83	260–262/257–259 (Mohammadi et al., 2012)
16			 6p	30	87	150–152/150–152 (Salimi et al., 2015)

^aReaction conditions: benzil (1 mmol), aldehydes (1 mmol), ammonium acetate (2 mmol), EtOH (3 ml), and Fe₃O₄@FU nanocomposite (12 mg) (**5a–k**).

^bReaction conditions: benzil (1 mmol), aldehydes (1 mmol), ammonium acetate (2 mmol), aniline (1 mmol), EtOH (3 ml), and Fe₃O₄@FU nanocomposite (12 mg) (**6l–p**).

^cIsolated yields.

^dThe ¹H NMR spectra for products 5a and 5c have been provided in supplementary file.

acknowledged that the chemical structure of the magnetic nanoparticles have been preserved after the functionalization.

Primarily, the size, structure, and morphology of FU, and the as prepared nanocomposite were investigated by SEM analyses

(Figures 2a,b). As can be seen, Fe₃O₄@FU nanocomposites have a cauliflower-shaped morphology in which the average size distribution was around 24–33 nm. TEM analysis of the as-synthesized Fe₃O₄@FU showed that the Fe₃O₄@FU NPs have a

core-shell structure (**Figure 2c**). Simultaneously, the elemental composition of $\text{Fe}_3\text{O}_4@FU$ and FU were studied by EDX analysis (**Figures 2d,e**) which confirmed the presence of O, C, Fe, and S elements constituted in the nanocomposite.

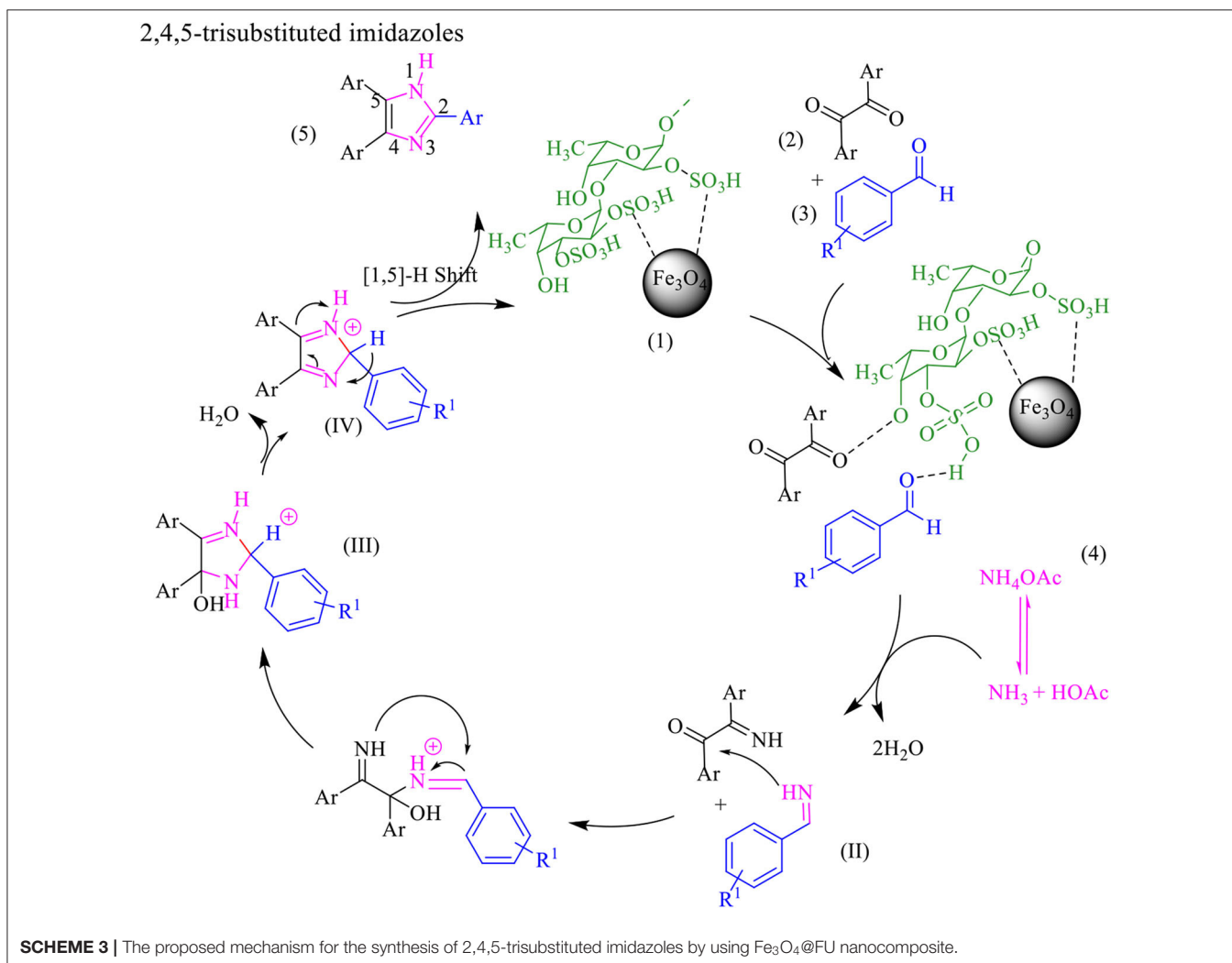
The surface area and pore size distributions of the $\text{Fe}_3\text{O}_4@FU$ were analyzed by N_2 adsorption-desorption analysis. As shown in **Figure 3**, $\text{Fe}_3\text{O}_4@FU$ NPs have type IV isotherms and type H_3 hysteresis loops. The BET surface area, average pore diameter and

the total pore volume were calculated to be $55.65 \text{ m}^2/\text{g}$, 11 nm , and $1.749 \text{ cm}^3/\text{g}$, respectively.

The XRD patterns of $\text{Fe}_3\text{O}_4@FU$ NPs are presented in **Figure 4**. As can be seen, diffraction peaks at 2θ values = 30.4° , 35.8° , 43.7° , 55.3° , 57.8° , and 63.3° could be indexed to the presence of all the crystal planes such as (220), (311), (400), (422), (511), and (440) attributed to the cubic inverse spinel structure of Fe_3O_4 which

TABLE 3 | Comparison of the activity of the catalysts in synthesis **5k** with some of the other catalysts reported in the literature.

Entry	Catalyst	Reaction condition	Reaction time (min)	Yield (%)	References
1	$[\text{Et}_3\text{NH}][\text{HSO}_4]$ (10 mol %)	Solvent-free/ 130°C	40	89	Deng et al., 2013
2	COPAPSC (20 mg)	Solvent-free/ 110°C	4h	77	Salimi et al., 2015
3	(CTA)3PMo-MMT nanocomposite (50 mg)	Solvent-free/ 100°C	60	85	Masteri-Farahani et al., 2020
4	$\text{Fe}_3\text{O}_4@FU$ (12 mg)	EtOH, Reflux	20	90	This work



matched with the standard pattern (JCPDS-PDF, No. 01-087-2334). These results proved that the crystalline structure of Fe_3O_4 was maintained after its decoration with fucoidan polysaccharide.

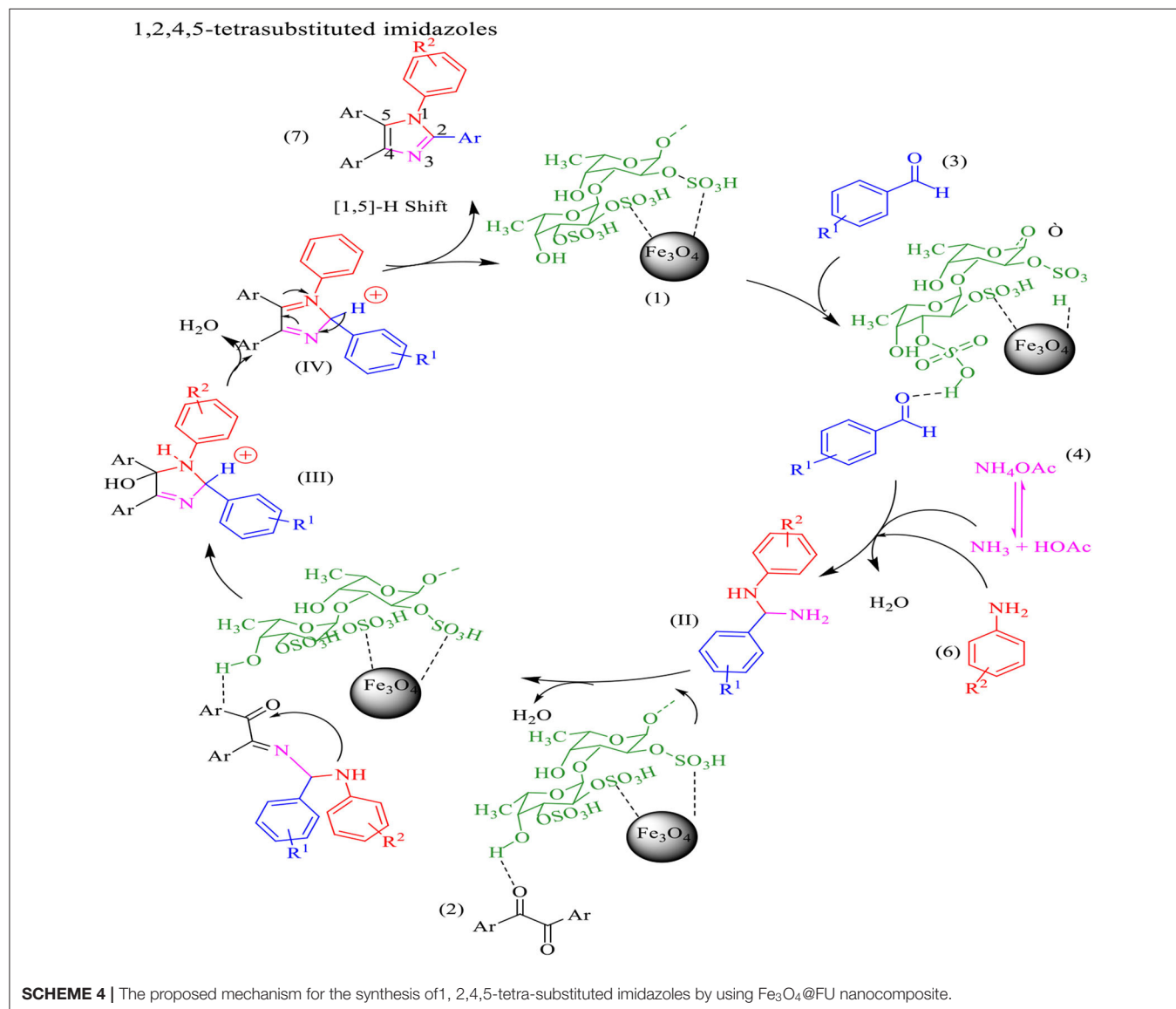
The magnetization curves of Fe_3O_4 and $\text{Fe}_3\text{O}_4@FU$ NPs measured at room temperature with a vibrating sample magnetometer (VSM) were shown in **Figure 5**. The hysteresis loops of $\text{Fe}_3\text{O}_4@FU$ NPs showed the superparamagnetic behavior of $\text{Fe}_3\text{O}_4@FU$ NPs. The saturation magnetization (M_s) values for the Fe_3O_4 and the $\text{Fe}_3\text{O}_4@FU$ NPs were 51, 35 emu/g, respectively. It is important to note that the saturation magnetization remains sufficient after covering by FU.

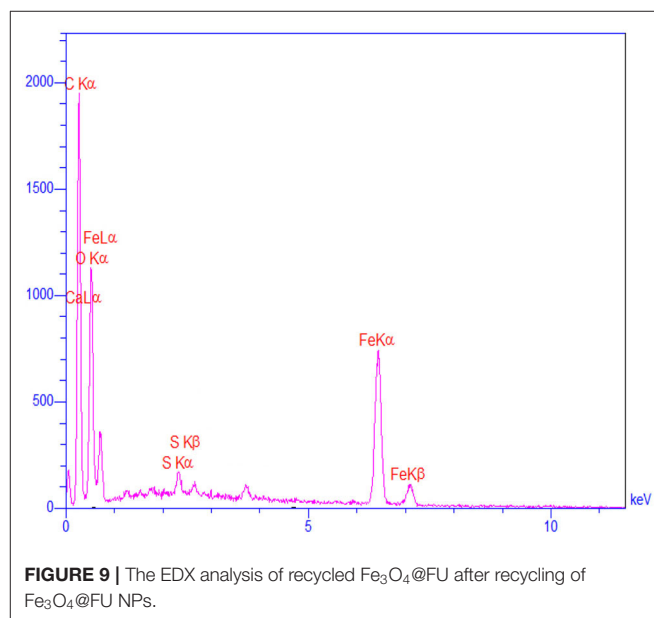
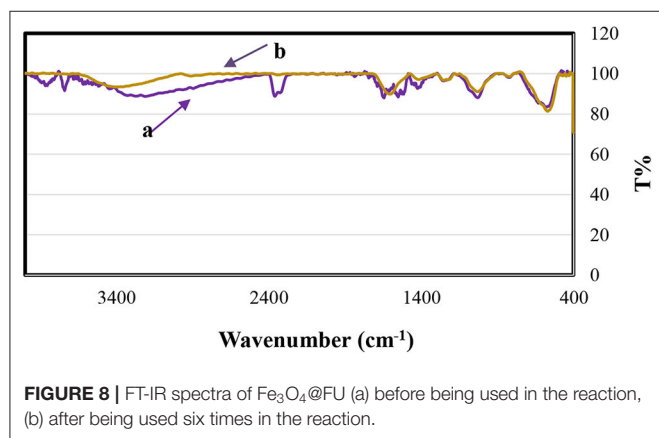
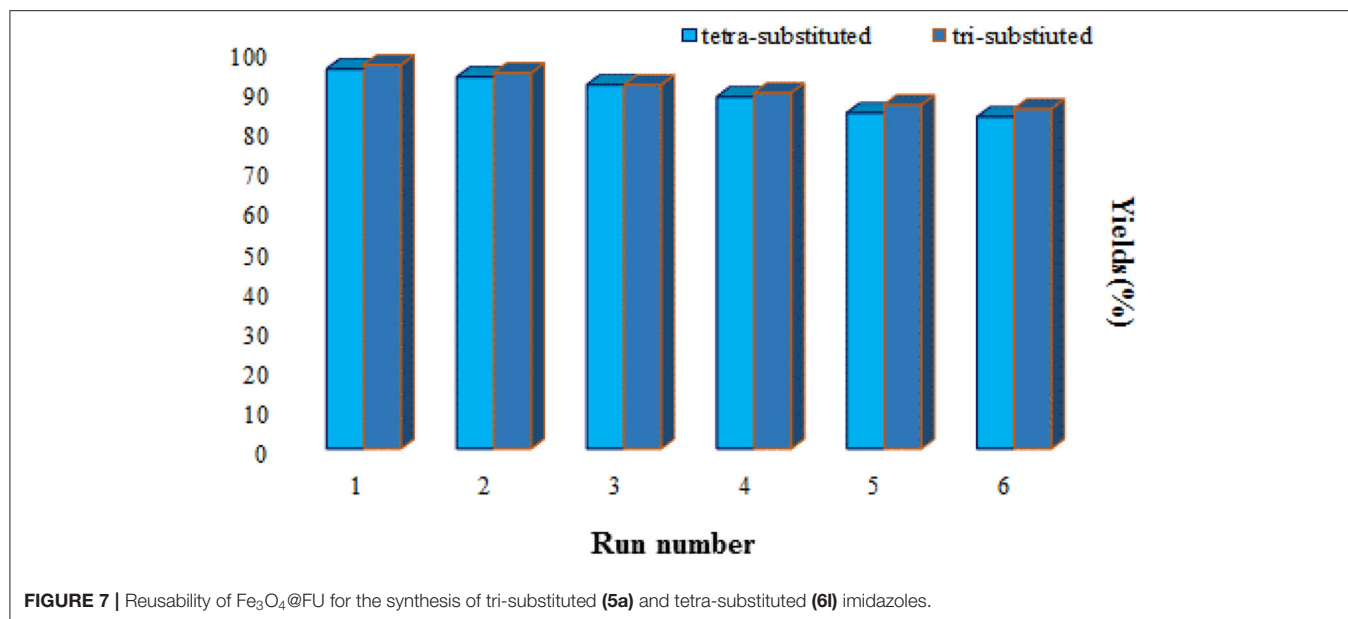
The thermogravimetric analysis (TGA) curve of FU and $\text{Fe}_3\text{O}_4@FU$ NPs showed three-stage weight loss in the temperature range from 100 to 500°C (**Figure 6**). The first weight loss of around 2 wt% ensues at 100°C indicating the evaporation of water or solvent. The next weight loss of about

12 wt% occurs at 240°C and the third weight loss about 42 wt% at 440°C for the decomposition of polysaccharide. Accordingly, the TGA studies showed improved stability for $\text{Fe}_3\text{O}_4@FU$ NPs.

Catalytic Activity of Magnetic $\text{Fe}_3\text{O}_4@FU$ NPs

The catalytic efficacy of $\text{Fe}_3\text{O}_4@FU$ NPs as a proficient heterogeneous catalyst was investigated in the one-pot reaction between benzil (1 mmol), benzaldehyde (1 mmol), and ammonium acetate (2 mmol) as a model reaction for the synthesis of imidazole derivatives. To determine the role of the catalyst, the model reaction was performed in the absence of the catalyst. The anticipated product was not shown after a long reaction time. The results reveal that the presence of the catalyst has a considerable effect on the formation of these compounds. The model reactions were carried out in the presence of different





solvents such as EtOH, H₂O, THF, and Toluene, CH₃CN and solvent-free conditions. As the results show, Ethanol (3 ml) was found to be the most effective solvent. To evaluate the optimum catalyst concentration, the model reaction was carried out in the presence of various amounts of catalyst (5, 10, 12, and 15 mg). Consequently, the best yield is accessible in the presence of just 12 mg catalyst, and use of extra amounts of the catalyst (15 mg) did not increase the result to a significant level (**Table 1**). The model reaction was carried out with FU, Fe₃O₄, and Fe₃O₄@FU. These results endorsed that Fe₃O₄@FU was more suitable for this reaction. Overall, the most significant conditions for the desired products were achieved at reflux under ethanol in the presence of 12 mg magnetic nanocomposite.

For total assessment of the synthesis of 2,4,5-trisubstituted and 1,2,4,5-tetrasubstituted imidazoles after the mentioned optimized conditions, various aromatic aldehydes and anilines were evaluated which can be seen in **Table 2**, including both electron-donating and electron-withdrawing substitutions which

were studied in these reactions. While the presence of electron-donating groups resulted in the corresponding products being prepared with lower reaction yields, in addition, electron-withdrawing functionalities led to the higher yields with shorter reaction times. Most of the products directly crystallized from the mixture of reaction with high purity with good to excellent yields (80–96%). It should be mentioned that all the products were confirmed by melting points, and some of the products were characterized by NMR spectral data.

To evaluate the generality of this catalyst in comparison to previously reported results in the literature, Fe₃O₄@FU acts as

an appropriate green biocatalyst due to the yields of products, reaction time and temperature (Table 3).

The proposed mechanism for the synthesis of tri-substituted imidazoles was shown in Scheme 3. In the first step, the aldehyde and benzil group were activated by the formation of a hydrogen bond with the functional group of fucoidan, followed by the nucleophilic attack of ammonia, coming from the ammonium acetate, the intermediate imine (II) is formed after the removal of H₂O. Intermediate (II) is then added to benzil forming intermediate (III). Dehydration of intermediate (III) afforded the intermediate (IV), which rearranges via 1,5 H-shift which, followed by deprotonation, gives tri substituted imidazole (5).

The proposed mechanism for the preparation of four one-pot reactions of benzil, aldehyde, and ammonium acetate and amine is shown in Scheme 4. Aldehyde and 1, 2-diketone were first activated by Fe₃O₄@FU, then amine was added to the aldehydes forming an imine intermediate which was attacked by ammonia (released from the ammonium acetate) to form the amine intermediate (II). On the other hand, the amine intermediate (II) reacted with the activated carbonyl groups of benzil to form the intermediate (III). Finally, the imidazole derivative was formed after dehydration, followed by a 1,5 H-shift.

The main concerns from an economic and environmental aspect, such as recyclability and the ability to reuse the catalyst, were also surveyed. In this regard, after the reaction was completed, the catalyst was collected by an external magnet and then washed with ethyl acetate, n-hexane and ethanol and dried at 50°C in an oven. The recycled catalyst was used six consecutive times in the reaction. According to the results, no appreciable reduction in the efficiency of the catalysts is observed (Figure 7).

The recycled catalyst was identified by EDX and FT-IR analysis. The comparison of the FT-IR spectrum of Fe₃O₄@FU before and after six consecutive runs confirms that no definite change in its structure was seen, which can therefore be considered as a recyclable and stable biocatalyst in organic reactions (Figure 8). However, the EDX analysis of the recovered

catalyst (Figure 9) showed that a degree of catalyst desulfation and leaching occurred after six runs, which explains the decrease in the yield of reactions.

CONCLUSION

In summary, magnetic core-shell structured fucoidan coated Fe₃O₄ NPs were *in situ* synthesized and their structural and magnetic properties were investigated. The catalytic property of Fe₃O₄@FU was studied in the synthesis of imidazoles derivatives. Outstanding catalytic activity alongside a simple synthesis method, easy processing and separation, a high product yield, and short reaction time make Fe₃O₄@FU an attractive bio-based heterogeneous catalyst.

DATA AVAILABILITY STATEMENT

The raw data supporting the conclusions of this article will be made available by the authors, without undue reservation.

AUTHOR CONTRIBUTIONS

MB and SA: investigation and writing—original draft preparation. SJ: project administration, conceptualization, resources, writing—review, and editing. All authors contributed to the article and approved the submitted version.

ACKNOWLEDGMENTS

The authors wish to express their gratitude for the partial financial support provided by the Research Council of Iran University of Science and Technology (IUST), Tehran, Iran.

SUPPLEMENTARY MATERIAL

The Supplementary Material for this article can be found online at: <https://www.frontiersin.org/articles/10.3389/fchem.2020.596029/full#supplementary-material>

REFERENCES

- Alipour, A., Javanshir, S., and Peymanfar, R. (2018). Preparation, characterization and antibacterial activity investigation of hydrocolloids based Irish moss/ZnO/CuO bio-based nanocomposite films. *J. Cluster Sci.* 29, 1329–1330. doi: 10.1007/s10876-018-1449-4
- Amirnejat, S., Movahedi, F., Masrouri, H., Mohadesi, M., and Kassaee, M. (2013). Silica nanoparticles immobilized benzoylthiourea ferrous complex as an efficient and reusable catalyst for one-pot synthesis of benzopyranopyrimidines. *J. Mol. Catal. A Chem.* 378, 135–141. doi: 10.1016/j.molcata.2013.05.023
- Amirnejat, S., Nosrati, A., and Javanshir, S. (2020c). Superparamagnetic Fe₃O₄@ Alginate supported L-arginine as a powerful hybrid inorganic–organic nanocatalyst for the one-pot synthesis of pyrazole derivatives. *Appl. Organomet. Chem.* 34:e5888. doi: 10.1002/aoc.5888
- Amirnejat, S., Nosrati, A., Javanshir, S., and Naimi-Jamal, M. R. (2020a). Superparamagnetic alginate-based nanocomposite modified by L-arginine: an eco-friendly bifunctional catalysts and an efficient antibacterial agent. *Int. J. Biol. Macromol.* 152, 834–845. doi: 10.1016/j.ijbiomac.2020.02.212
- Amirnejat, S., Nosrati, A., Peymanfar, R., and Javanshir, S. (2020b). Synthesis and antibacterial study of 2-amino-4H-pyrans and pyrans annulated heterocycles catalyzed by sulfated polysaccharide-coated BaFe₁₂O₁₉ nanoparticles. *Res. Chem. Intermed.* 46, 3683–3701. doi: 10.1007/s11164-020-04168-x
- Dekamin, M. G., Peyman, S. Z., Karimi, Z., Javanshir, S., Naimi-Jamal, M. R., and Barikani, M. (2016). Sodium alginate: an efficient biopolymeric catalyst for green synthesis of 2-amino-4H-pyran derivatives. *Int. J. Biol. Macromol.* 87, 172–179. doi: 10.1016/j.ijbiomac.2016.01.080
- Deng, X., Zhou, Z., Zhang, A., and Xie, G. (2013). Brønsted acid ionic liquid [Et 3 NH][HSO 4] as an efficient and reusable catalyst for the synthesis of 2, 4, 5-triaryl-1H-imidazoles. *Res. Chem. Intermed.* 39, 1101–1108. doi: 10.1007/s11164-012-0669-8
- Dolatkhah, Z., Javanshir, S., Bazgir, A., and Hemmati, B. (2019). Palladium on magnetic Irish moss: a new nano-biocatalyst for suzuki type cross-coupling reactions. *Appl. Organomet. Chem.* 33:e4859. doi: 10.1002/aoc.4859
- Dolatkhah, Z., Javanshir, S., Bazgir, A., and Mohammadkhani, A. (2018). Magnetic isinglass a nano-bio support for copper immobilization: Cu-IG@ Fe₃O₄ a heterogeneous catalyst for triazoles synthesis. *ChemistrySelect* 3, 5486–5493. doi: 10.1002/slct.201800501

- Fereshteh, N., and Shahrzad, J. (2020). Magnetic $\gamma\text{Fe}_2\text{O}_3@ \text{Sh}@ \text{Cu}_2\text{O}$: an efficient solid-phase catalyst for reducing agent and base-free click synthesis of 1, 4-disubstituted-1, 2, 3-triazoles. *BMC Chem.* 14:9. doi: 10.1186/s13065-019-0657-9
- Gadekar, L. S., Mane, S. R., Katkar, S. S., Arbad, B. R., and Lande, M. K. (2009). Scolecite as an efficient heterogeneous catalyst for the synthesis of 2, 4, 5-triarylimidazoles. *Cent. Eur. J. Chem.* 7, 550–554. doi: 10.2478/s11532-009-0050-y
- Gomez-Zavaglia, A., Prieto Lage, M. A., Jimenez-Lopez, C., Mejuto, J. C., and Simal-Gandara, J. (2019). The potential of seaweeds as a source of functional ingredients of prebiotic and antioxidant value. *Antioxidants* 8:406. doi: 10.3390/antiox8090406
- Graebn, C. S., Ribeiro, F. V., Rogério, K. R., and Kümmerle, A. E. (2019). Multicomponent reactions for the synthesis of bioactive compounds: a review. *Curr. Org. Synth.* 16, 855–899. doi: 10.2174/1570179416666190718153703
- Hemmati, B., Javanshir, S., and Dolatkah, Z. (2016). Hybrid magnetic Irish moss/ Fe_3O_4 as a nano-biocatalyst for synthesis of imidazopyrimidine derivatives. *RSC Adv.* 6, 50431–50436. doi: 10.1039/C6RA08504K
- Karimi, A. R., Alimohammadi, Z., Azizian, J., Mohammadi, A. A., and Mohammadzadeh, M. (2006). Solvent-free synthesis of tetrasubstituted imidazoles on silica gel/ NaHSO_4 support. *Catal. Commun.* 7, 728–732. doi: 10.1016/j.catcom.2006.04.004
- Marques, M. V., Ruthner, M. M., Fontoura, L. A., and Russowsky, D. (2012). Metal chloride hydrates as Lewis acid catalysts in multicomponent synthesis of 2, 4, 5-triarylimidazoles or 2, 4, 5-triarylloxazoles. *J. Braz. Chem. Soc.* 23, 171–179. doi: 10.1590/S0103-50532012000100024
- Masteri-Farahani, M., Ezabadi, A., Mazarei, R., Ataieina, P., Shahsavarifar, S., and Mousavi, F. (2020). A new nanocomposite catalyst based on clay-supported heteropolyacid for the green synthesis of 2, 4, 5-trisubstituted imidazoles. *Appl. Organomet. Chem.* 34:e5727. doi: 10.1002/aoc.5727
- Mirsafaei, R., Heravi, M. M., Ahmadi, S., and Hosseinnejad, T. (2016). Synthesis and properties of novel reusable nano-ordered KIT-5-N-sulfamic acid as a heterogeneous catalyst for solvent-free synthesis of 2, 4, 5-triaryl-1 H-imidazoles. *Chem Pap.* 70, 418–429. doi: 10.1515/chempap-2015-0228
- Mohammadi, A., Keshvari, H., Sandaroos, R., Maleki, B., Rouhi, H., Moradi, H., et al. (2012). A highly efficient and reusable heterogeneous catalyst for the one-pot synthesis of tetrasubstituted imidazoles. *Appl. Catal. A.* 429, 73–78. doi: 10.1016/j.apcata.2012.04.011
- Momahed Heravi, M., Karimi, N., and Pooremami, S. (2019). One-pot three components synthesis of 2, 4, 5-triaryl-imidazoles catalyzed by Caro's acid-silica gel under solvent-free condition. *Adv. J. Chem. A.* 2, 73–78. doi: 10.29088/SAMI/AJCA.2019.2.7378
- Piri, T., Peymanfar, R., Javanshir, S., and Amirnejat, S. (2019). Magnetic $\text{BaFe}_{12}\text{O}_{19}/\text{Al}_2\text{O}_3$: an efficient heterogeneous lewis acid catalyst for the synthesis of α -aminophosphonates (Kabachnik–Fields Reaction). *Catal. Lett.* 149, 3384–3394. doi: 10.1007/s10562-019-02910-8
- Pourian, E., Javanshir, S., Dolatkah, Z., Molaei, S., and Maleki, A. (2018). Ultrasonic-assisted preparation, characterization, and use of novel biocompatible core/shell $\text{Fe}_3\text{O}_4@ \text{GA}@$ isinglass in the synthesis of 1, 4-dihydropyridine and 4 H-pyran derivatives. *ACS Omega* 3, 5012–5020. doi: 10.1021/acsomega.8b00379
- Ray, S., Das, P., Bhaumik, A., Dutta, A., and Mukhopadhyay, C. (2013). Covalently anchored organic carboxylic acid on porous silica nano particle: a novel organometallic catalyst (PSNP-CA) for the chromatography-free highly product selective synthesis of tetrasubstituted imidazoles. *Appl. Catal. A.* 458, 183–195. doi: 10.1016/j.apcata.2013.03.024
- Sadeghi, B., Mirjalili, B. B. F., and Hashemi, M. M. (2008). BF_3SiO_2 : an efficient reagent system for the one-pot synthesis of 1, 2, 4, 5-tetrasubstituted imidazoles. *Tetrahedron Lett.* 49, 2575–2577. doi: 10.1016/j.tetlet.2008.02.100
- Salimi, M., Nasser, M. A., Chapesshloo, T. D., and Zakerinasab, B. (2015). (Carboxy-3-oxopropylamino)-3-propylsilylcellulose as a novel organocatalyst for the synthesis of substituted imidazoles under solvent-free conditions. *RSC Adv.* 5, 33974–33980. doi: 10.1039/C5RA01909E
- Shaabani, A., Afshari, R., and Hooshmand, S. E. (2017). Crosslinked chitosan nanoparticle-anchored magnetic multi-wall carbon nanotubes: a bio-nanoreactor with extremely high activity toward click-multi-component reactions. *New J. Chem.* 41, 8469–8481. doi: 10.1039/C7NJ01150D
- Shaabani, A., Sepahvand, H., Hooshmand, S. E., and Borjian Boroujeni, M. (2016). Design, preparation and characterization of $\text{Cu}/\text{GA}/\text{Fe}_3\text{O}_4@ \text{SiO}_2$ nanoparticles as a catalyst for the synthesis of benzodiazepines and imidazoles. *Appl. Organomet. Chem.* 30, 414–421. doi: 10.1002/aoc.3448
- Shalini, K., Sharma, P. K., and Kumar, N. (2010). Imidazole and its biological activities: a review. *Der Chemica Sinica* 1, 36–47.
- Shaterian, H. R., and Ranjbar, M. (2011). An environmental friendly approach for the synthesis of highly substituted imidazoles using Bronsted acidic ionic liquid, N-methyl-2-pyrrolidonium hydrogen sulfate, as reusable catalyst. *J. Mol. Liq.* 160, 40–49. doi: 10.1016/j.molliq.2011.02.012
- Shitole, B. V., Shitole, N. V., Ade, S. B., and Kakde, G. K. (2015). Microwave-induced one-pot synthesis of 2, 4, 5-trisubstituted imidazoles using rochelle salt as a green novel catalyst. *Orbital Electron. J. Chem.* 7, 240–244. doi: 10.17807/orbital.v7i3.720
- Varzi, Z., and Maleki, A. (2019). Design and preparation of $\text{ZnS}-\text{ZnFe}_2\text{O}_4$: a green and efficient hybrid nanocatalyst for the multicomponent synthesis of 2, 4, 5-triaryl-1H-imidazoles. *Appl. Organomet. Chem.* 33:e5008. doi: 10.1002/aoc.5008
- Zaheri, H. M., Javanshir, S., Hemmati, B., Dolatkah, Z., and Fardpour, M. (2018). Magnetic core-shell Carrageenan moss/ Fe_3O_4 : a polysaccharide-based metallic nanoparticles for synthesis of pyrimidinone derivatives via Biginelli reaction. *Chem. Cent. J.* 12:108. doi: 10.1186/s13065-018-0477-3
- Zayed, A., and Ulber, R. (2019). Fucoidan production: approval key challenges and opportunities. *Carbohydr. Polym.* 211, 289–297. doi: 10.1016/j.carbpol.2019.01.105
- Zayed, A., and Ulber, R. (2020). Fucoidans: downstream processes and recent applications. *Mar. Drugs* 18:170. doi: 10.3390/md18030170
- Zheng, Y., Monty, J., and Linhardt, R. J. (2019). Polysaccharide-based nanocomposites and their applications. *Carbohydr. Res.* 405, 23–32. doi: 10.1016/j.carres.2014.07.016

Conflict of Interest: The authors declare that the research was conducted in the absence of any commercial or financial relationships that could be construed as a potential conflict of interest.

Copyright © 2020 Banazadeh, Amirnejat and Javanshir. This is an open-access article distributed under the terms of the Creative Commons Attribution License (CC BY). The use, distribution or reproduction in other forums is permitted, provided the original author(s) and the copyright owner(s) are credited and that the original publication in this journal is cited, in accordance with accepted academic practice. No use, distribution or reproduction is permitted which does not comply with these terms.